Title: Magnetic molecularly imprinted polymers based on attapulgite/Fe_3O_4 particles for the selective recognition of 2,4-dichlorophenol

Authors: Jianming Pan, Longcheng Xu, Jiangdong Dai, Xiuxiu Li, Hui Hang, Pengwei Huo, Chunxiang Li, Yongsheng Yan

PII: S1385-8947(11)00992-2
DOI: doi:10.1016/j.cej.2011.08.046
Reference: CEJ 8335

To appear in: *Chemical Engineering Journal*

Received date: 31-5-2011
Revised date: 16-8-2011
Accepted date: 16-8-2011

Please cite this article as: J. Pan, L. Xu, J. Dai, X. Li, H. Hang, P. Huo, C. Li, Y. Yan, Magnetic molecularly imprinted polymers based on attapulgite/Fe_3O_4 particles for the selective recognition of 2,4-dichlorophenol, *Chemical Engineering Journal* (2010), doi:10.1016/j.cej.2011.08.046

Magnetic molecularly imprinted polymers based on attapulgite/Fe_3O_4 particles for the selective recognition of 2,4-dichlorophenol

Jianming Pan, Longcheng Xu, Jiangdong Dai, Xiuxiu Li, Hui Hang, Pengwei Huo, Chunxiang Li*, Yongsheng Yan
School of Chemistry and Chemical Engineering, Jiangsu University, Zhenjiang 212013, China

ABSTRACT

Via encapsulation of attapulgite/Fe_3O_4 magnetic particles (ATP/Fe_3O_4), the magnetic molecularly imprinted polymers (MMIPs) were synthesized for the selective recognition of 2,4-dichlorophenol (2,4-DCP). MMIPs were charcterized by X-ray diffraction (XRD), Fourier transform infrared (FT-IR) analysis, thermogravimetric analysis (TGA), vibrating sample magnetometer (VSM), transmission electron microscopy (TEM), nitrogen adsorption-desorption analysis and Raman spectroscopy. MMIPs were demonstrated claviform shape with an imprinted polymer film (thickness of about 16 nm), and exhibited magnetic property (M_s = 5.67 emug^{-1}) and thermal stability. Batch mode adsorption studies were carried out to investigate the specific binding capacity, binding kinetics and recognition specificity. The Langmuir isotherm model was fitted to the equilibrium data better than the other models, and the monolayer adsorption capacity of MMIPs were 145.79 mg g^{-1} at 298 K. The kinetic properties of MMIPs were well described by the pseudo-second-order equation, initial adsorption rate and half-adsorption time. The selective recognition experiments demonstrated high affinity and selectivity towards 2,4-DCP over structurally related phenolic compounds. In addition, MMIPs could be regenerated, and their adsorption capacity in the fifth use was about 7.53% loss in 2,4-DCP solution. The MMIPs as-prepared were successfully applied to the separation of 2,4-DCP from environmental water samples.

Keywords Surface imprinted polymers; Selective recognition; 2,4-dichlorophenol; Attapulgite/Fe_3O_4 magnetic particles; Magnetic susceptibility

1. Introduction

Molecular imprinting is a powerful technique to make imprinted cavities within a polymer network [1]. Its product, molecularly imprinted polymers (MIPs), have been utilized for a wide variety of applications, including in chromatography [2], solid phase extraction [3], drug controlled release and sensor devices [4], where the MIPs function as a recognition element. By preparing the MIPs film on a solid support substrate, surface-imprinting technique provides an alternative way to improve mass transfer and reduce permanent entrapment of the template [5]. Attapulgite (ATP), possessing of the ideal molecular formula of $[Si_8Mg_5O_{20}(OH)_2(H_2O)_4{\cdot}4H_2O$, is a kind of hydrated octahedral layered magnesium aluminum silicate mineral with the fibrous morphology [6]. In our previous investigation, ATP has been successfully applied in surface imprinting process owing to its fibrous morphology, special structure, high surface area, stable

* Corresponding author Tel.: +86-0511-88790683; fax: +86-0511-88791800.
E-mail address: pjm@ujs.edu.cn (C.X. Li)

chemical properties and large reserves in China [7, 8].

Compared with conventional solid support substrate, magnetic nanoparticles (MNPs) have been received increasing attention on synthesizing magnetic molecularly imprinted polymers (MMIPs). Due to the high magnetic susceptibility of MNPs, MMIPs binding target molecules can be easily collected and separated by an external magnetic field without additional centrifugation or filtration, which makes separation easier and faster [9]. Moreover, MMIPs, prepared by coating MNPs with MIPs, can not only selectively recognize the template molecules in the complex matrix, but also possessed more imprinted cavities within the polymer network because of high surface-to-volume ratio of MNPs [10, 11]. Therefore, when combining MNPs with MIPs, MMIPs could be the promising multifunctional candidate for the selective separation of trace analyses at an external magnetic field [12, 13]. More recently, Fe_3O_4 magnetic particles were widely used in surface imprinting process [10].

Chlorophenols, such as 2,4-dichlorophenol (2,4-DCP), are very common and have been listed in the priority pollutants into the aquatic environment [14]. Their sources are wastewater as a consequence of industrial and agricultural activities, including petroleum refineries, plastics, rubbers, pharmaceuticals, wood-preserving and steel industries [15]. Also, some chlorophenols may be carcinogenic in nature owing to their toxicity, stability and bioaccumulation [16]. Discharge of chlorophenol contaminated wastewater into aquatic environment without adequate treatment can lead to negative effect on the water quality, and pose a serious ecological problem as mutagenic effects on the living [15, 17]. In addition, 2,4-DCP is one of the most environmentally representative chlorophenols because it is used extensively in the manufacture of pesticides and herbicides such as 2,4-dichlorophenoxiacetic acid [18]. Thus, selective separation and removal of 2,4-DCP from complex matrix is of great importance.

To avoid leakage of Fe_3O_4 particles and fragility of the resultant MMIPs, this work was to synthesize attapulgite/Fe_3O_4 magnetic particles (ATP/Fe_3O_4) by co-precipitation technique in the aqueous suspension of attapulgite pre-modified with $FeCl_3$ [19]. And then ATP/Fe_3O_4 magnetic particles, possessing special structure, stable properties and low-cost, were coated with a thin MIPs film. This film was obtained using 2,4-DCP as a template, methacrylic acid (MAA) as functional co-monomers, 2,2´-Azobisisobutyronitrile (AIBN) as a initiator and ethyl glycol dimethacrylate (EGDMA) as a cross-linker. Synthesis route of MMIPs and their application for removal of 2,4-DCP with the help of an applied magnetic field were shown in Fig. 1. The characterization, binding capacity, kinetics, selectivity and regeneration of these MMIPs were investigated. Finally, MMIPs were used as sorbent for the solid phase extraction (SPE) and determination of 2,4-DCP from environmental water samples.

2. Materials and methods

2.1. Materials

ATP was supplied by Aotebang International Co. in China. Prior to use, it was activated by calcination at 350 ^{o}C for 6.0 h before it was dispersed in 0.1 M NH_4Cl for 4.0 h at room temperature. MAA, iron(II) chloride tetrahydrate ($FeCl_2{\cdot}4H_2O$), iron(III) chloride hexahydrate ($FeCl_3{\cdot}6H_2O$), oleic acid, acetonitrile, methyl sulfoxide (DMSO), HPLC-grade methanol were obtained from Sinopharm Chemical Reagent Co.,

Ltd. (Shanghai, China). Ethyl glycol dimethacrylate (EGDMA) (Shanghai Xingtu Chemical Co. Ltd., Shanghai, China) was washed consecutively with 10% aqueous NaOH, water and brine, dried over $MgSO_4$, filtered and then distilled under reduced pressure. 2,2´-Azobisisobutyronitrile (AIBN) (Shanghai No.4 Reagent & H.V. Chemical Co. Ltd., Shanghai, China) was recrystallized from methanol prior to use. 2,4-DCP, 2,6-dichlorophenol (2,6-DCP), Bisphenol A (BPA), 2,4,6-trichlorophenol (TCP), 4-chlorophenol (4-CP) and polyvinylpyrrolidone (PVP) were all purchased from Aladdin reagent CO., LTD (Shanghai, China).

2.2. Synthesis of attapulgite/Fe_3O_4 magnetic particles (ATP/Fe_3O_4)

The synthetic process of attapulgite/Fe_3O_4 magnetic particles was followed a modified coprecipitation method [19]. As follows: $FeCl_3 \cdot 6H_2O$ (4.72 g) was added into 180 ml of deionized ultrapure water, and 2.1 g of ATP was dispersed into the mixture in ultrasonic bath for 30 min. Next, the mixture was stirred for 3.0 h, and a stable suspension was obtained. Then $FeCl_2 \cdot 4H_2O$ (1.72 g) was dissolved in the suspension with vigorous stirring (800 rpm) under nitrogen. When the solution temperature was increased to 80 ^oC, 10 mL of NH_4OH (25%, w/w) added drop by drop under stirring, and the reaction was maintained for 30 min. The black precipitate was separated by putting the vessel on a Nd-Fe-B permanent magnet, and washed several times. Finally, the black product ATP/Fe_3O_4 magnetic particles were dried in the vacuum.

2.3. Synthesis of 2,4-DCP imprinted MNPs (MMIP)

The MMIPs were prepared followed the literature [20] with a few modifications. 2,4-DCP (1.0 mmol), MAA (6.0 mmol) were dispersed into the 10 mL of DMSO in ultrasonic bath for 1.0 h. This step was to preparation of the preassembly solution. The ATP/Fe_3O_4 particles (1.5 g) were mixed with 1.5 mL of oleic acid and stirred for 10 min. Then 20 mmol of EGDMA and the preassembly solution were added into the mixture of ATP/Fe_3O_4 and oleic acid. This mixture was stirred (300 rpm) continually for 30 min to obtain the prepolymerization solution. Moreover, the PVP (0.4 g) used as dispersant was dissolved into 100 mL of DMSO:water (9:1, v/v) in a threenecked round-bottomed flask under stirring. Then the prepolymerization solution was added into the three-necked flask, and then 0.3 g of AIBN was also added into it. The mixture was stirred at 300 rpm and purged with nitrogen gas to displace oxygen while the temperature increased to 60 ^oC. The reaction was allowed to proceed at 60 ^oC for 24 h. After the polymerization, the obtained polymers were washed with the mixture solution of methanol/acetic acid (95:5, v/v) using soxhlet extraction to remove the template molecules. Finally, the obtained MMIPs were dried at 50 ^oC under vacuum. In comparison, the magnetic non-imprinted polymers (MNIPs) were also prepared as a blank in parallel but without the addition of 2,4-DCP.

2.4. Characterization of MMIPs

Infrared spectra (4000–400 cm^{-1}) was recorded on a Nicolet NEXUS-470 FTIR apparatus (U.S.A.). Raman spectra was recorded in the range of 200–2000 cm^{-1} at ambient temperature using a WITEC Spectra Pro 2300I spectrometer equipped with an Ar-ion laser, which provided a laser beam of 514 nm wavelength.

The identification of crystalline phase was performed using a Rigaku D/max-γB X-ray diffract meter (XRD) with monochromatized with Cu Kα radiation over the 2θ range of 20–80° at a scanning rate of 0.02 deg s^{-1}. The morphology of MMIPs was observed by transmission electron microscope (TEM, JEOL IEM-200CX). Magnetic measurements were carried out using a VSM (7300, Lakeshore) under a magnetic field up to 10 kOe. Thermogravimetric analysis (TGA) was performed for powder samples (about 10 mg) using a Diamond TG/DTA instruments (PerkinElmer, USA) under a nitrogen atmosphere up to 600 ^{o}C with a heating rate of 5.0 ^{o}C min^{-1}. High performance liquid chromatograph (HPLC) analysis was performed on a Shimadzu LC-20A system (Shimadzu, Kyoto, Japan) equipped with a UV-vis detector (set at 285 nm). The injection loop volume was 20 μL, and the mobile phase consisted of deionized ultrapure water and methanol with a volume ratio of 40 : 60. The flow rate of the mobile phase was 1.0 mL min^{-1}. The oven temperature was set at 25 ^{o}C. A TBS-990 atomic absorption spectrophotometer (Beijing Purkinge General Instrument Co. Ltd, Beijing, China) with a deuterium background correction and a GF990 graphite furnace atomizer systemwas used. Specific surface area and pore size were measured using a NOVA2000e analytical system made by Quantachrome Corporation (USA).

2.5. Batch mode binding studies

The experimental parameters such as pH, contact time, initial concentration of 2,4-DCP and temperature on the adsorption of 2,4-DCP were studied in a batch mode of operations. For this purpose, a certain amount of sorbent (MMIPs or MNIPs) was dispersed in testing solution of 2,4-DCP (10 mL). After the desired time, the MMIPs and MNIPs were isolated by an external magnetic field, and the concentration of 2,4-DCP in the solvent phase was determined with UV-vis spectrophotometer. Moreover, the equilibrium adsorption capacity (Q_e, mg g^{-1}) was calculated.

The adsorption equilibrium was then fitted to Langmuir and Freundlich isotherm model. The linear form of the Langmuir isotherm model is expressed by the following equation:

$$\frac{C_e}{Q_e} = \frac{1}{Q_m K_L} + \frac{C_e}{Q_m} \qquad (1)$$

where C_e is the equilibrium concentration of adsorbate (mg L^{-1}), Q_e is the equilibrium adsorption capacity (mg g^{-1}), Q_m is the maximum adsorption capacity of the adsorbent, K_L is the affinity constant.

The linear form of the Freundlich isotherm model is given as follow:

$$\ln Q_e = \ln K_F + (1/n) \ln C_e \qquad (2)$$

where K_F (mg g^{-1}) and n are the adsorption equilibrium constants.

The kinetic data obtained were analyzed using pseudo-first-order rate equation and pseudo-second-order rate equation. The pseudo-first-order equation can be expressed as Eq.(3).

$$\ln\left(Q_e - Q_t\right) = \ln Q_e - k_1 t \qquad (3)$$

The pseudo-second-order equation can be expressed as Eq.(4).

$$\frac{t}{Q_t} = \frac{1}{K_2 Q_e^2} + \frac{t}{Q_e} \qquad (4)$$

where Q_e and Q_t are the amount of adsorbate (mg g^{-1}) onto adsorbent at the equilibrium and time t (min), respectively. Values of k_1 (L min^{-1}) and k_2 (g mg^{-1} min^{-1}) are calculated from the plot of $\ln(Q_e - Q_t)$ versus t and t/q_t versus t, respectively.

2.6. Selective recognition experiments.

To measure the selective recognition for 2,4-DCP, 10 mg of the MMIPs or MNIPs were added into 25 mL flasks, each of which contained 10 mL solution with 100 mg L^{-1} of 4-CP, 2,4-DCP, 2,6-DCP, TCP and bisphenol A, respectively. The initial solution pH was adjusted to 6.0 and the experiments were carried out on a shaker at 25 ^{o}C for 3.0 h.

The distribution coefficients (K_d), selectivity coefficients (k) and relative selectivity coefficient (k') of 4-CP, 2,6-DCP, TCP and BPA with respect to 2,4-DCP can be obtained according to Eqs. 5 to 7.

$$K_d = Q_e / C_e \quad (5)$$

In Eq. 5, K_d (L g^{-1}) represents the distribution coefficient; Q_e (mg g^{-1}) and C_e (mg L^{-1}) represents the adsorption capacity and equilibrium concentration of the each phenolic compound, respectively. The selectivity coefficient (k) for binding of a specific phenolic compound can be obtained according to the following equation:

$$k = K_{d(2,4\text{-DCP})}/K_{d(X)} \quad (6)$$

$K_{d(2,4\text{-DCP})}$ and $K_{d(X)}$ are the distribution coefficient for 2,4-DCP and its structural analogs, respectively. A relative selectivity coefficient k' can be defined as Eq. 7. k_M and k_N are the selectivity coefficients of MMIPs and MNIPs, respectively.

$$k' = k_M/k_N \quad (7)$$

2.7. Magnetite leakage studies

In order to estimate the amount of magnetite that is likely to leach from the MMIPs, 100 mg of the MMIPs were placed in test tubes containing 10 ml of 50% (v/v) acetic acid solution and were shaken by a rotary shaker for 12 h. The amount of the magnetite leached into leach media was determined by a graphite furnace atomic absorption spectrophotometer.

2.8. Sample preparation and SPE procedure

Water samples were obtained from Yangtse Rive, Yudai River and tap water, Zhenjiang, China. Freshly collected water samples were immediately filtered through a millipore cellulose nitrate membrane (pore size was 0.45 mm) to remove suspended particles. Then the pH of the water samples was adjusted to 6.0 with diluted HCl and diluted NH_4OH before SPE.

50 mg of MMIPs were put into a beaker and then 250 mL of water samples with spiked concentration ranging from 50 μg L^{-1} to 200 μg L^{-1} were added into the beaker and the mixture was stirred for 2.0 h at 25 ^{o}C. Then the MMIPs with adsorbed 2,4-DCP were separated rapidly from the solutions by Nd-Fe-B permanent magnet. Subsequently, the supernatant solutions were discarded and the MMIPs were transferred into a testing bottle and were washed with 2×2.0 mL of acetonitrile. Finally, the 2,4-DCP were desorbed from the MMIPs with 2×2.5 mL of methanol solution containing 5.0% acetic under the action of ultrasound.

The extracts were combined and evaporated to dryness under nitrogen gas at 40 ^{o}C, and the residues were dissolved with 2.0 mL of 20% aqueous methanol for further HPLC analysis.

3. Results and discussions

3.1. Characterization of MMIPs and MNIPs

The infrared spectra of the ATP/Fe_3O_4 (a) and MMIPs (b) were measured and shown in Fig. 2A, respectively. The main functional groups of the predicted structure can be observed with corresponding infrared absorption peaks. The absorption bands at 587 cm^{-1} and 445 cm^{-1} of MMIPs corresponded to the Fe-O bond for spinel Fe_3O_4 particles, which was also obtained for ATP/Fe_3O_4 [19]. The characteristic bands of Si-O-Si for ATP/Fe_3O_4 and MMIPs were observed around 1042 cm^{-1}. The MMIPs showed the strong absorption bands ataround 1725, 1260 and 1156 cm^{-1}, which were assigned to C=O stretching vibration of carboxyl (MAA), C–O symmetric and asymmetric stretching vibration of ester (EGDMA), respectively [21]. The characteristic peak of C-Cl bond stretching vibration was shown at 668 cm^{-1} [22]. The peaks at 2987 cm^{-1} and 2928 cm^{-1} of MMIPs, which were absent in ATP/Fe_3O_4, indicated the presence of C–H stretching bands of both -CH_3 and -CH_2 groups. The absorption band at 3440 cm^{-1} of the MMIPs could be attributed to the stretching vibration of O-H bonds from MAA molecules. All the results confirmed that the co-polymerization of MAA and EGDMA on the surface ATP/Fe_3O_4 in the presence of AIBN has been initialed.

In order to effectively distinguish the maghemite or magnetite nanoparticles on the surface of ATP, the Raman spectroscopy of ATP/Fe_3O_4 (a) and MMIPs (b) in the wave length range of 250-850 cm^{-1} was shown in Fig. 2B. Several broad peaks around 305, 515 and 672 cm^{-1} were observed in ATP/Fe_3O_4 and MMIPs. Those peaks were typical Raman peaks of Fe_3O_4, which can be assigned to Eg, T2g and A1g mode of Fe_3O_4 [23]. In addition, few miscellaneous peaks could be assigned to the trace amounts of maghemite resulting from oxidation of Fe_3O_4 to Fe_2O_3 during the imprinting process.

The morphology of ATP/Fe_3O_4 and MMIPs were observed by TEM. As can be observed in Fig. 3a, the thickness of raw ATP particles was 42±8.0 nm, and the small size of Fe_3O_4 particles (black particles) was 10 nm on average. Due to the negative surface charges, iron cations can be bonded onto the surface of ATP via electrostatic forces easily [19]. Then the Fe_3O_4 particles obtained by co-precipitation process dispersed onto the ATP surface. From the morphology of MMIPs (Fig. 3b), the rough surface with black particles (Fe_3O_4 particles) were shown. According to the thickness of MMIPs (75±9.0 nm), the thickness of the imprinted film for MMIPs was almost 16 nm, which may be benefit for the fast extraction equilibrium within a short time. The specific surface area, total pore volume and average pore diameter for MMIPs and MNIPs were listed in Table Supporting Information (Table SI1). The results indicated that MMIPs exhibitted a more porous surface than that of MNIPs. But the parameters of MNIPs were not obviously different from those of MNIPs. Therefore, the distinct adsorption properties for MMIPs and MNIPs could not entirely be attributed to the morphological differences such as porous surface, but to the imprinting effect.

Fig. 4 showed the thermogravimetric analysis (TGA) of the ATP/Fe_3O_4, MMIPs and MNIPs. As shown in Fig. 4, the first weight loss stage can be ascribed to the evaporation of water molecules for each particle,

which were 5.38%, 2.92% and 4.36% for ATP/Fe_3O_4, MMIPs and MNIPs, respectively [24]. The second weight loss stage started at 250 ^oC and 300 ^oC for MNIPs and MMIPs, respectively. In this stage, there were no significant differences of the mass loss of the MMIPs and MNIPs were observed, which were 50.39% and 50.58% for MMIPs and MNIPs, respectively. Compared with MMIPs and MNIPs, ATP/Fe_3O_4 can not be easily decomposed at high temperatures, which showed little weight loss (8.10% below 600 ^oC). Thus, the remaining mass for MMIPs and MNIPs were attributed to the thermal resistance of ATP/Fe_3O_4 particles, and the quantity of ATP/Fe_3O_4 particles in the MMIPs and MNIPs were 46.69% and 44.04%, respectively, indicating the MMIPs and MNIPs possessed of similar morphological structure and size distribution [25].

Fig. 5a showed the magnetic hysteresis loop analysis of ATP/Fe_3O_4, MMIPs and MNIPs, respectively. It was obviously that there was similar general shape and trend of the three curves, indicating three particles were superparamagnetic [26]. The saturation magnetization (Ms) values obtained at room temperature were 13.23 $emug^{-1}$, 5.67 $emug^{-1}$ and 5.12 $emug^{-1}$ for ATP/Fe_3O_4, MMIPs and MNIPs, respectively. Because of the small particle surface effect such as magnetically inactive layer containing spins that were not collinear with the magnetic field, the Ms values for three particles were lower than that of theoretical value for magnetite which was 92 $emug^{-1}$ [27, 28]. Moreover, the results from Fig. 5b strongly suggested that the remained magnetic force in MMIPs could be attracted by an external magnetic field effectively. The results also illustrated that MMIPs was a feasible magnetic separation carrier. By magnetite leakage studies, no magnetite was determined from MMIPs, suggesting that MMIPs prevented magnetite leakage successfully.

Fig. 6 showed the X-ray diffraction (XRD) patterns of ATP/Fe_3O_4 (a), MMIPs (b) and MNIPs (c). In the 2θ range of 20°-70°, six characteristic peaks corresponded to Fe_3O_4 (2θ=30.23°, 35.54°, 43.10°, 53.50°, 57.23°, and 62.82°) were observed in the ATP/Fe_3O_4, MMIPs and MNIPs, and the peak positions could be indexed to (220), (311), (400), (422), (511) and (440) (JCPDS card (19-0629) for Fe_3O_4). The results suggested that the addition of raw ATP particles or polymers into Fe_3O_4 did not change its crystalline form. Moreover, it also could be seen that the XRD patterns of MMIPs and MNIPs were similar to that of ATP/Fe_3O_4, indicating they had the same cylinder wall structure and interplanner spacing.

3.2. Effect of pH for adsorption medium

Optimization of pH value for adsorption medium plays a vital role in the adsorption studies. The pH of the solution affects the degree of ionization and speciation of dichlorophenols which subsequently leads to a change in adsorption kinetics and equilibrium characteristics [29]. Then, the effect of pH on the adsorption of 2,4-DCP and the effect of initial pH on final pH were shown in Fig. 7. It was observed that adsorption of 2,4-DCP at pH 2.0 and 6.0 did not cause any change in pH. Fig. 7 also showed that adsorption of neutral 2,4-DCP at pH 2.0 and 6.0 was the optimal condition for MMIPs and MNIPs. The fact neutral molecules of dichlorophenol are benefit for the adsorption process has also been reported previously for other sorbent by Sathishkumar et al. [30]. Due to the real pH value approaching to 7.0 was favourable for 2,4-DCP separation and detection from environmental water samples, pH 6.0 for adsorption medium was selected in the following studies. Moreover, the initial pH had the same effects for MMIPs and MNIPs, but the adsorption capacity for MMIPs was more than that of MNIPs, strongly indicating the imprinting effect.

3.3. Binding properties and Scatchard analysis

The binding properties of MMIPs and MNIPs for 2,4-DCP were studied by the static equilibrium adsorption, and the corresponding adsorption isotherms were shown in Fig. 8. From Fig. 8, when the equilibrium concentration increased, the equilibrium adsorption capacity (Q_e) for 2,4-DCP firstly increased sharply, then increased slightly, and finally reached to maximum point, as expected. The 2,4-DCP adsorbed on MMIPs was greater than that of MNIPs, indicating the significantly preferential adsorption of 2,4-DCP for MMIPs. It was probably because MMIPs illustrated the good specificity for the imprinted molecule. By fitting the experimental data with Langmuir and Freundlich isotherm equations (Fig. 9), it was also found that Langmuir isotherm model fitted the equilibrium data significantly better than that of Freundlich model, indicating monolayer molecular adsorption for MMIPs and MNIPs.

In order to further study the specificity, Scatchard plot was used to discuss the binding characteristics [31]. Scatchard equation as following:

$$Q_e/C_e = (Q_{max} - Q_e)/K_{di} \qquad (8)$$

where K_{di} (mg L^{-1}) is the dissociation constant of binding sites; Q_{max} (mg g^{-1}) is the maximum amount of apparent binding; C_e (mg L^{-1}) is the equilibrium concentration of 2,4-DCP in testing solution; Q_e is the equilibrium adsorption capacity. Scatchard graph was plotted based on Eq. (8) (inset of Fig. 8).

As shown in Scatchard plot of MMIPs (Fig. 8), the relationship between Q_e/C_e and Q_e was not a single linear curve, but consisted of two linear parts with different slopes, which suggested that there were two kinds of different binding sites existed in MMIPs. This kind of non-intervalence-type molecular imprinting polymer has been reported by the other researchers [10, 31]. The linear equations corresponding to two linear relationships were $Q_e/C_e=-0.0173Q_e+1.8986$ in the range of 12.60–50.71mg g^{-1} and $Q_e/C_e=-0.0076Q_e+1.6649$ in the range of 77.71–150.99 mg g^{-1}. The K_{di} and Q_{max} were calculated from the slops and intercepts, and they were 57.80 mg L^{-1} and 109.75 mg g^{-1} for the high affinity sites, and 131.58 mg L^{-1} and 219.07 mg g^{-1} for the low affinity sites, respectively. The binding of 2,4-DCP to the MNIPs was also analyzed by Scatchard method. It revealed homogeneous binding sites with K_{di} and Q_{max} values of 120.48 mg L^{-1} and 130.60 mg g^{-1}, respectively.

3.4. Binding kinetics

The adsorption rate constants and linear regression values from two rate equations were summarized in Table 1. Based on the second-order model, the initial adsorption rate (h, mg g^{-1} min^{-1}) and half equilibrium time ($t_{1/2}$, min) were also listed in Table 1 according to the following equations [32]:

$$h = K_2 Q_e^2 \qquad (9)$$

$$t_{1/2} = \frac{1}{K_2 Q_e} \qquad (10)$$

The adsorption of 2,4-DCP followed pseudo-second-order kinetics well because of the favourable fit between experimental and calculated values of Q_e (R^2 values above 0.99). And it was assumed that chemical process could be the rate-limiting step in the adsorption process for 2,4-DCP [33]. Moreover, with the increase of temperature and initial concentration, the initial adsorption rate and adsorption capacity

increased obviously. It was possible that the initial concentration of 2,4-DCP molecules provided the necessary driving force to overcome the resistances of mass transfer between the aqueous phases and the solid phase [34]. Furthermore, higher temperature may provided more chances for 2,4-DCP molecules to pass the external boundary layer, and produced the enlargement of pore volume and surface area enabling dichlorophenol molecules to penetrate further [17, 35]. The adsorption kinetic curves of MMIPs and MNIPs at different temperatures and initial concentrations were shown in Figure Supporting Information 1 (Figure SI1). It was evidential that a much higher adsorption capacity was achieved on MMIPs. A comparison of the values of h and $t_{1/2}$, MMIPs offered a fast kinetics for the adsorption of 2,4-DCP than those of MNIPs. After the quick adsorption, the adsorption process reached nearly to equilibrium at 45 min with different removal efficiency for MMIPs and MNIPs. It could be attributed to the fact that intraparticle diffusions for 2,4-DCP was not impeded to the same extent when the presence of imprinted binding sites.

3.5. Selectivity of MMIPs

To further evaluate the specificity of MMIPs, TCP, 2,6-DCP, BPA and 4-CP, as the structural analogs, were carried out for the adsorption specifiicity experiment. Values of K_d, k and k' were summarized in Table 2. From the data in Table 2, the following facts could be found: (i) The k values of MMIPs presented significant increase than those of MNIPs, showing that MMIPs had the highest molecular recognition selectivity to 2,4-DCP. (ii) k' is an indicator to express the adsorption affinity of recognition sites to the template molecules. The k' results showed that the selectivity of MMIPs was more than twice as high as MNIPs. (iii) The values of k' were 3.487, 2.318, 4.379 and 4.838 for 4-CP, 2,6-DCP, TCP and BPA, respectively, indicating the recognition for 2,4-DCP and its structural analogs followed the order 2,4-DCP>BPA>TCP>4-CP>2,6-DCP. Although the same hydrogen bond can form between the structural analogs and MAA, the different recognition effect may be based on the distinct size, structure and functional group to the template [36]. Moreover, 2,6-DCP has nearly the same structure as 2,4-DCP, but the equilibrium concentration of 2,4-DCP by MMIPs was still much lower than that for 2,6-DCP, suggesting that the memory of specific functional group also plays an important role in the conformation menory [37]. The results suggested that the imprinting process significantly improved adsorption selectivity to the imprinted template.

Table 10 summaries the comparison of the adsorption properties for phenolic compounds on different sorbents reported in the literatures [38-41]. Evidently, the binding capacity of the MMIPs for template was excellent, but the recognition specificity were not superior to many traditional imprinted sorbents. However, MMIPs based on attapulgite/Fe_3O_4 particles possessed of many advantages, such as collected and separation process was more convenient. Especially, it could be used as intelligent material to respond to magnetic field. Compared with MMIPs based on Kaolinite/Fe_3O_4, MMIPs based on attapulgite/Fe_3O_4 particles exhibited excellent thermal stability and saturation magnetization due to the claviform morphology of ATP [41].

3.6. Regeneration of MMIPs and analysis of environmental water samples

To test the regeneration of the MMIPs, five adsorption/desorption (regeneration) cycles were conducted with 2,4-DCP. The mixture of methanol and acetic acid (9.5:0.5,V/V) was used as a eluant. After the supernatant solution was discarded, the MMIPs were washed with 2×2.5 mL of eluant under ultrasonic bathe for 30 min. From the results in Figure SI2, after five cycles of regeneration, the adsorption capacity of MMIPs for 2,4-DCP was about 7.5% loss in 2,4-DCP solution, suggesting good retention of the activity of the MMIPs.

To demonstrate the applicability of the method, several water samples were analyzed. The recovery study was carried out by spiking environmental water samples. The recoveries from 76.3±8.1 to 95.5±4.9% were obtained for 2,4-DCP (Table 4). The results indicated that the proposed method was applicable for the separation and determination of 2,4-DCP in different environmental water samples.

4. Conclusions

In this work, the attapulgite/Fe_3O_4 magnetic nanoparticles, possessing of special structure, stable chemical properties and low-cost, were synthesized by co-precipitation technique. Then we developed an efficient method for synthesis of magnetic molecularly imprinted polymers using attapulgite/Fe_3O_4 magnetic particles as support. The prepared MMIPs exhibited excellently specific recognition, thermal stability and saturation magnetization. It could be easily separated from the suspension by an external magnetic field, leading to a fast and selective recognition of 2,4-DCP from aqueous solutions. After MMIPs were reused and regenerated five times, the fifth adsorption capacity was still excellent. We believe that these surface-imprinted polymers with magnetic composites as supports can be one of the most promising candidates for environmental pollutants separation.

Acknowledgment. This work was financially supported by the National Natural Science Foundation of China (No.21077046, No.30970309) and Ph.D. Programs Foundation of Ministry of Education of China (No. 20093227110015).

Supporting Information Available: Adsorption kinetic curves of MMIPs and MNIPs at different temperatures and initial concentrations. Stability and potential regeneration of the MMIPs after five cycles.

References and notes.

[1] Jackson, R., Petrikovics, I., Lai, E.P.C., Yu, J.C.C., *Anal. Methods* 2 (2010) 552-557.
[2] Kim, K., Kim, D., *J. Appl. Polym. Sci.* 96 (2005) 200-212.
[3] Scorrano, S., Longo, L., Vasapollo, G., *Anal. Chim. Acta* 659 (2010) 167-171.
[4] Chuang, S.W., Rick, J., Chou, T.C., *Biosens. Bioelectron*. 24 (2009) 3170-3173.
[5] Gao, B.J., Wang, J., An, F.Q., Liu, Q., *Polymer* 49 (2008) 1230-1238.
[6] Shi, L.M., Yao, J.F., Jiang, J.L., Zhang, L.X., Xu, N.P., Microporous Mesoporous Mater. 122 (2009) 294-300.
[7] Pan, J.M., Zou, X.H., Wang, X., Guan, W., Yan, Y.S., Han, J., *Chem. Eng. J.* 162 (2010) 910-918.

[8] Pan, J.M., Zou, X.H., Yan, Y.S., Wang, X., Guan, W., Han, J., Wu, X.Y., *Appl. Clay Sci.* 50 (2010) 260-265.

[9] Jing, T., Du, H.R., Dai, Q., Xia, H., Niu, J.W., Hao, Q.L., Mei, S.R., Zhou, Y.K., *Biosens. Bioelectron.* 26 (2010) 301-306.

[10] Chen, L.G., Liu, J., Zeng, Q.L., Wang, H., Yu, A.M., Zhang, H.Q., Ding, L., *J. Chromatogr. A* 1216 (2009) 3710-3719.

[11] Wang, H.F., He, Y., Ji, T.R., Yan, X.P., *Anal. Chem.* 81 (2009) 1615-1621.

[12] Zhou, W.H., Lu, C.H., Guo, X.C., Chen, F.R., Yang, H.H., Wang, X.R., *J. Mater. Chem.* 20 (2010) 880-883.

[13] Tan, C.J., Tong, Y.W., *Anal. Chem.* 79 (2007) 299-306.

[14] Kieth, L.H., Telliard, W.A., *Environ. Sci. Technol.* 13 (1979) 416-423.

[15] Li, Y., Li, X., Li, Y.Q., Qi, J.Y., Bian, J., Yuan, Y.X., *Environ. Pollut.* 157 (2009) 1879-1885.

[16] Shen, X.T., Zhu, L.H., Liu, G.X., Yu, H.W., Tang, H.Q., *Environ. Sci. Technol.* 42 (2008) 1687-1692.

[17] Pan, J.M., Zou, X.H., Wang, X., Guan, W., Li, C.X., Yan, Y.S., Wu, X.Y., *Chem. Eng. J.* 166 (2011) 40-48.

[18] Puyol, D., Mohedano, A.F., Sanz, J.L., Rodríguez, J.J., *Chemosphere* 76 (2009) 1192-1198.

[19] Liu, Y.S., Liu, P., Su, Z.X., Li, F.S., Wen, F.S., *Appl. Surf. Sci.* 255 (2008) 2020-2025.

[20] Chen, L.G., Zhang, X.P., Sun, L., Xu, Y., Zeng, Q.L., Wang, H., Xu, H.Y., Yu, A.M., Zhang, H.Q., Ding, L., *J. Agric. Food Chem.* 57 (2009) 10073-10080.

[21] Yoshimatsu, K., Reimhult, K., Krozer, A., Mosbach, K., Sode, K., Ye, L., *Anal. Chim. Acta* 584 (2007) 112-121.

[22] Li, Y., Li, X., Chu, J., Dong, C.K., Qi, J.Y., Yuan, Y.Y., *Environ. Pollut.* 158 (2010) 2317-2324.

[23] Wu, X., Tang, J.Y., Zhang, Y.C., Wang, H., *Mater. Sci. Eng., B* 157 (2009) 81-86.

[24] Feng, B., Hong, R.Y., Wang, L.S., Guo, L., Li, H.Z., Ding, J., Zheng, Y., Wei, D.G., *Colloids Surf., A* 328 (2008) 52-59.

[25] Zhan, Y., Liu, R.J., Hu, Y.L., Li, G.K., *Anal. Chem.*, 81(2009) 967-976.

[26] Wang, X., Wang, L.Y., He, X.W., Zhang, Y.K., Chen, L.X., *Talanta* 78 (2009) 327-332.

[27] Zaitsev, V.S., Filimonov, D.S., Presnyakov, I.A., Gambino, R.J., Chu, B., *J. Colloid Interface Sci.* 212 (1999) 49-57.

[28] Kodama, R.H., Berkowitz, A.E.Jr., Mcniff, E.J., Foner, S., *Phys. Rev. Lett.* 77 (1996) 394-397.

[29] Sathishkumar, M., Binupriya, A.R., Kavitha, D., Selvakumar, R., Jayabalan, R., Choi, J.G., Yun, S.E., *Chem. Eng. J.* 147 (2009) 265-271.

[30] Mazzotti, M., *J. Chromatogr. A.* 1126 (2006) 311-322.

[31] Gu, X.H., Xu, R., Yuan, G.L., Lu, H., Gu, B.G., Xie, H.P., *Anal. Chim. Acta* 675 (2010) 64-70.

[32] Wu, Z.J., Joo, H., Lee, K., *Chem. Eng. J.* 112 (2005) 227-236.

[33] Baydemir, G., Andac, M., Bereli, N., Say, R., Denizli, A., *Ind. Eng. Chem. Res.* 46 (2007) 2843-2852.

[34] Mazzotti, M., *J. Chromatogr. A* 1126 (2006) 311-322.

[35] Alqodah, Z., *Water Res.* 34 (2000) 4295-4303.

[36] Chang, Y., Ko, T., T. Hsu, Syu, M., *Anal. Chem.*, 2009, 81, 2098-2105.

[37] Yu Q., Deng S.B., Yu G., *Water Res.*, 2008, 42, 3089-3097.

[38] Yang, K.G., Liu, Z.B., Mao, M., Zhang, X.H., Zhao, C.S., Norio, N., *Anal. Chim. Acta* 2005, 546, 30-36.

[39] An, F.Q., Gao, B.J., Feng, X.Q., *J. Hazard. Mater.* 2008, 157, 286-292.

[40] Wang, X., Pan, J.M., Guan, W., Dai, J.D., Zou, X.H., Yan, Y.S., Li, C.X., Hu, W., *J. Chem. Eng. Data* 2011, 56, 2793-2801.

[41] Guo, W.L., Hu, W., Pan, J.M, Zhou, H.C., Guan, W., Wang, X., Dai, J.D., Xu, L.C., *Chem. Eng. J.* 2011, 171, 603-611.

Legends to the figures:

Fig.1 Synthesis route of MMIPs and their application for removal of 2,4-DCP with the help of an applied magnetic field.

Fig. 2 (A) FT-IR spectrum of the ATP/Fe_3O_4 (a) and MMIPs (b). (B) Raman spectrum of the ATP/Fe_3O_4 (a) and MMIPs (b)

Fig. 3 Micrographs from a transmission electron microscope of ATP/Fe_3 (a) and MMIPs (b).

Fig. 4 Thermogravimetric analysis of the ATP/Fe_3O_4, MMIPs and MNIPs.

Fig. 5 (a) Magnetization curves at 298K of ATP/Fe_3O_4, MMIPs and MNIPs. (b) A photograph of MMIPs suspended in water in the absence (left image) and in the presence (right) of an externally placed magnet.

Fig. 6 X-ray diffraction (XRD) patterns of ATP/Fe_3O_4 (a), MMIPs (b) and MNIPs (c).

Fig. 7 Effect of pH on adsorptive removal of 2,4-DCP. Inset: Effect of initial pH on equilibrium pH. Temperature: 298 K, sorbent dose: 0.01 g, solution volume: 10.0 mL, contact time: 2.0 h, initial concentration: 100 mg L^{-1}.

Fig. 8 The adsorption isotherms and the Scatchard plots of MMIPs and MNIPs (inset). Temperature: 298 K, sorbent dose: 0.01 g, solution volume: 10.0 mL, contact time: 2.0 h, pH value: 6.0.

Fig. 9 Fitting the experimental data with Langmuir and Freundlich (inset) isotherm equations.

Legends to the tables:

Table 1 Kinetic constants for the Pseudo-first-order equation and Pseudo-second-order equation. Temperature: 298 K, sorbent dose: 0.01 g, solution volume: 10.0 mL, contact time: 2.0 h, initial concentration: 100 mg L^{-1}, pH value: 6.0.

Table 2 Adsorption selectivity of MMIPs and MNIPs. Temperature: 298 K, sorbent dose: 0.01 g, solution volume: 10.0 mL, contact time: 3.0 h, initial concentration: 100 mg L^{-1}, pH value: 6.0.

Table 3 Comparison of the adsorption properties for phenolic compounds on different sorbents.

Table 4 The intra- and inter-day precisions and recoveries of the assay (n = 6). Temperature: 298 K, sorbent dose: 0.05 g, solution volume: 250 mL, contact time: 2.0 h, pH value: 6.0.

Legends to the supporting information:

Figure SI1 Adsorption kinetic curves of MMIPs and MNIPs at different temperatures and initial concentrations.

Temperature: 298 K, sorbent dose: 0.01 g, solution volume: 10.0 mL, contact time: 2.0 h, initial concentration: 100 mg L^{-1}, pH value: 6.0.

Figure SI2 Stability and potential regeneration of the MMIPs after five cycles.

Temperature: 298 K, sorbent dose: 0.01 g, solution volume: 10.0 mL, contact time: 2.0 h, initial concentration: 100 mg L^{-1}, pH value: 6.0.

Table SI1 Comparison of MMIPs and MNIPs from nitrogen adsorption-desorption analysis.

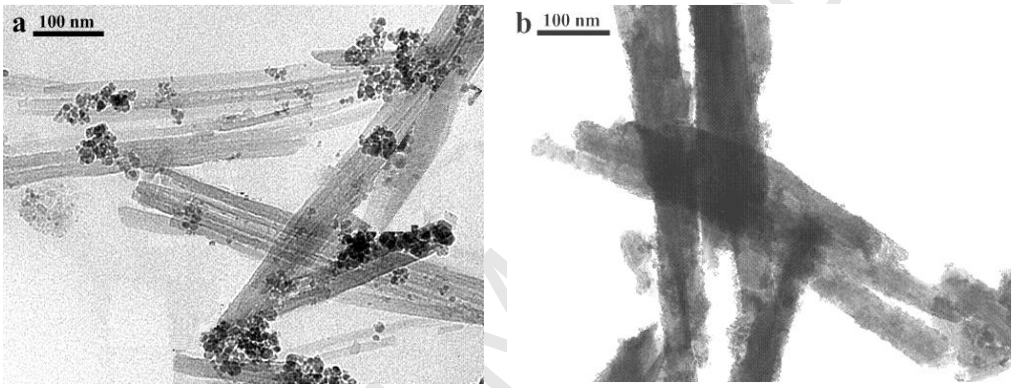

Research Highlights

1. **ATP/Fe_3O_4 magnetic nanoparticles were synthesized by co-precipitation technique.**
2. **ATP/Fe_3O_4 magnetic particles were coated with a thin MIPs film.**
3. **MMIPs could avoid leakages of Fe_3O_4 particles and fragility of the resultant MMIPs.**
4. **Structural characteristics, binding properties and imprinting mechanism were discussed in details.**
5. **Binding capacity, kinetics, selectivity and regeneration of the MMIPs were investigated.**

Table 1 Kinetic constants for the Pseudo-first-order equation and Pseudo-second-order equation.

Adsorbates	C_0 (mg L^{-1})	T (K)	$Q_{e,exp}$ (mg g^{-1})	Pseudo-first-order equation			Pseudo-second-order equation				
				$Q_{e,c}$ (mg g^{-1})	k_1 (L min^{-1})	R^2	$Q_{e,c}$ (mg g^{-1})	$k_2\times10^{-3}$ (g mg^{-1} min^{-1})	h (mg g^{-1} min^{-1})	$t_{1/2}$ (min)	R^2
MMIPs	100	298	41.84	16.35	0.0335	0.9328	43.29	4.64	8.11	5.16	0.9993
	100	308	43.34	19.33	0.0394	0.9821	45.04	4.29	8.05	5.38	0.9993
	150	298	74.10	21.95	0.0167	0.9861	75.19	7.53	41.33	1.79	0.9999
MNIPs	100	298	33.64	18.50	0.0494	0.9855	35.46	4.91	5.56	6.05	0.9977
	100	308	34.76	17.13	0.0451	0.9782	36.23	5.28	6.38	5.45	0.9995
	150	298	58.76	16.77	0.0641	0.9683	59.88	9.14	31.57	1.86	0.9999

Table 2 Adsorption selectivity of MMIPs and MNIPs.

Phenolic compounds	MMIPs			MNIPs			k'
	C_e (mg L^{-1})	K_d (L g^{-1})	k	C_e (mg g^{-1})	K_d (L g^{-1})	k	
2,4-DCP	42.27	1.366	_	75.52	0.324	_	_
4-CP	70.43	0.420	3.253	74.21	0.347	0.933	3.487
2,6-DCP	55.45	0.803	1.693	69.25	0.444	0.730	2.318
TCP	69.68	0.435	3.126	68.77	0.454	0.714	4.379
BPA	79.20	0.263	5.179	76.76	0.303	1.070	4.838

Table 3 Comparison of the adsorption properties for phenolic compounds on different sorbents.

Template	Sorbent	Q_{max} (mg g^{-1})	k'	Reference
2,4-DCP	Imprinted microspheres based on cyclodextrin/attapulgite	62.14	6.07-11.0	[7]
BPA	Imprinted- polyethersulfone microspheres	9.590	1.03-4.36	[38]
Phenol	MIP-PEI/SiO_2	46.60	39.0-40.7	[39]
3-Chlorophenol	Imprinted popolymer based on KH-570/SiO_2 composites	163.7	4.33-5.23	[40]
BPA	Magnetic imprinted polymers based on Kaolinite/Fe_3O_4	112.4	3.81-17.3	[41]
2,4-DCP	Magnetic imprinted polymers based on attapulgite/Fe_3O_4	145.79	2.32-4.84	This work

Table 4 The intra- and inter-day precisions and recoveries of the assay (n = 6).

Water samples	Intra-day precision						Inter-day precision					
	50 μg L^{-1}		**100 μg L^{-1}**		**200 μg L^{-1}**		**50 μg L^{-1}**		**100 μg L^{-1}**		**200 μg L^{-1}**	
	Recovery (%)	**RSD (%)**	**Recovery (%)**	**RSD (%)**	**Recovery (%)**	**RSD (%)**	**Recovery (%)**	**RSD (%)**	**Recovery (%)**	**RSD (%)**	**Recovery (%)**	**RSD (%)**
Yangtse Rive	**88.7**	**5.7**	**90.5**	**6.2**	**95.5**	**4.9**	**85.3**	**3.7**	**87.4**	**2.4**	**94.4**	**3.7**
Yudai River	**77.5**	**5.1**	**84.9**	**4.2**	**85.4**	**5.2**	**76.3**	**8.1**	**78.4**	**6.6**	**83.1**	**4.5**
Tap water	**83.6**	**3.6**	**88.1**	**5.1**	**89.3**	**4.5**	**82.9**	**6.3**	**84.5**	**4.9**	**83.5**	**9.3**

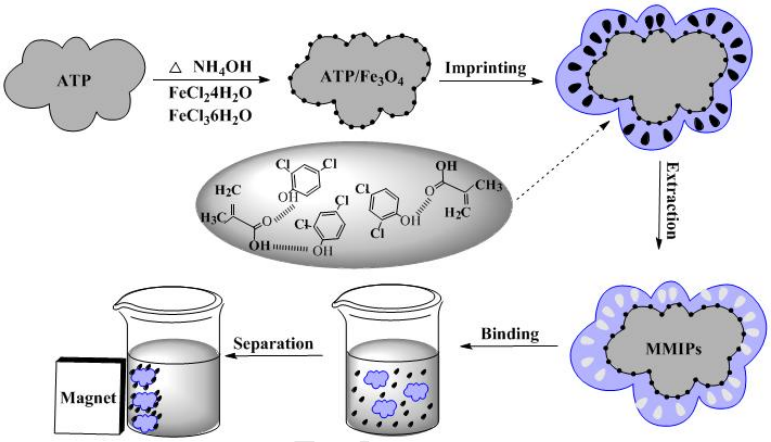

Fig.1 Synthesis route of MMIPs and their application for removal of 2,4-DCP with the help of an applied magnetic field.

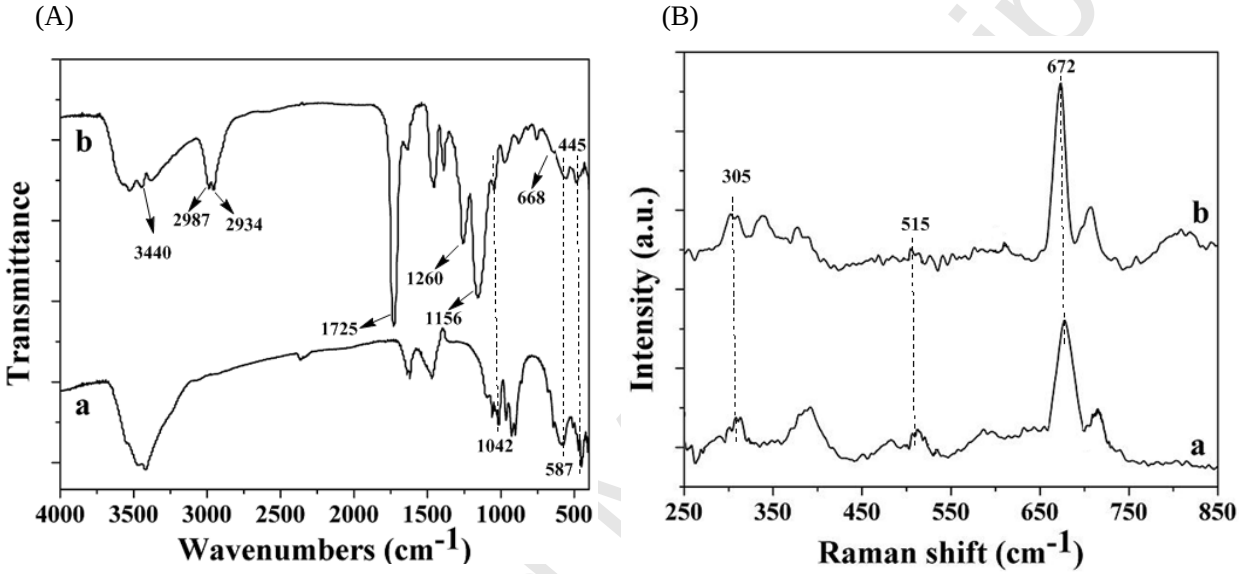

Fig. 2 (A) FT-IR spectrum of the ATP/Fe_3O_4 (a) and MMIPs (b). (B) Raman spectrum of the ATP/Fe_3O_4 (a) and MMIPs (b)

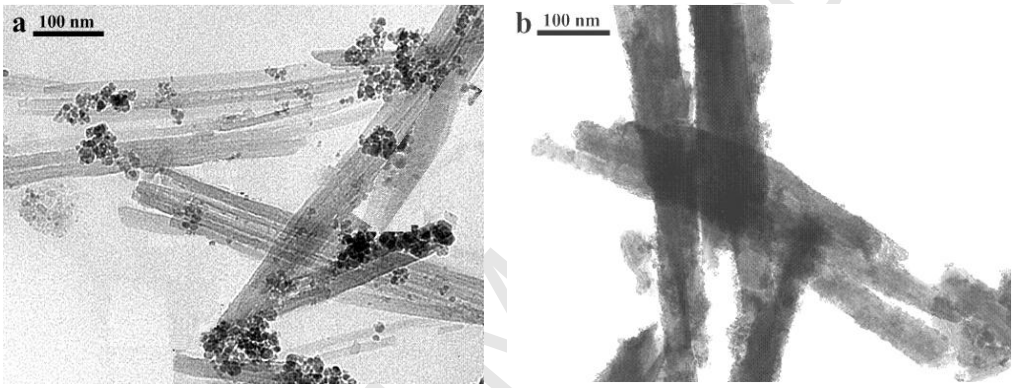

Fig. 3 Micrographs from a transmission electron microscope of ATP/Fe_3O_4 (a) and MMIPs (b).

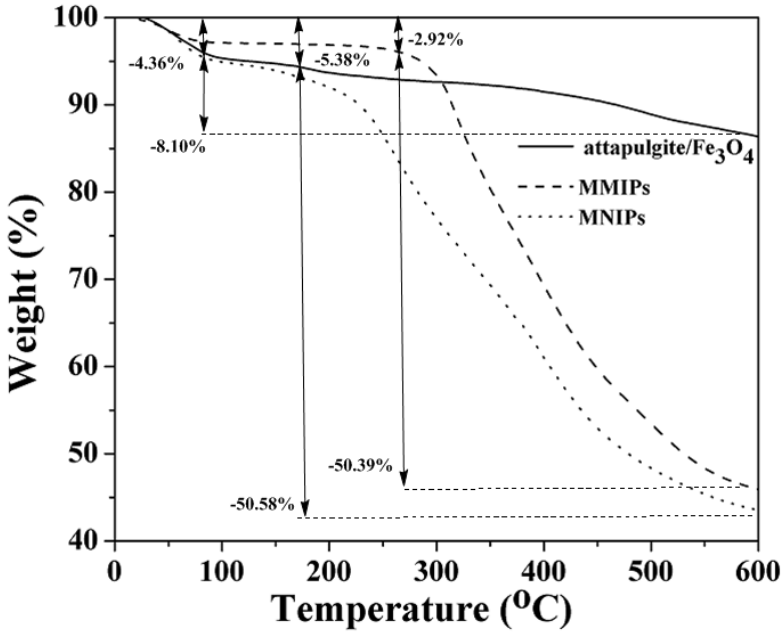

Fig. 4 Thermogravimetric analysis of the ATP/Fe_3O_4, MMIPs and MNIPs.

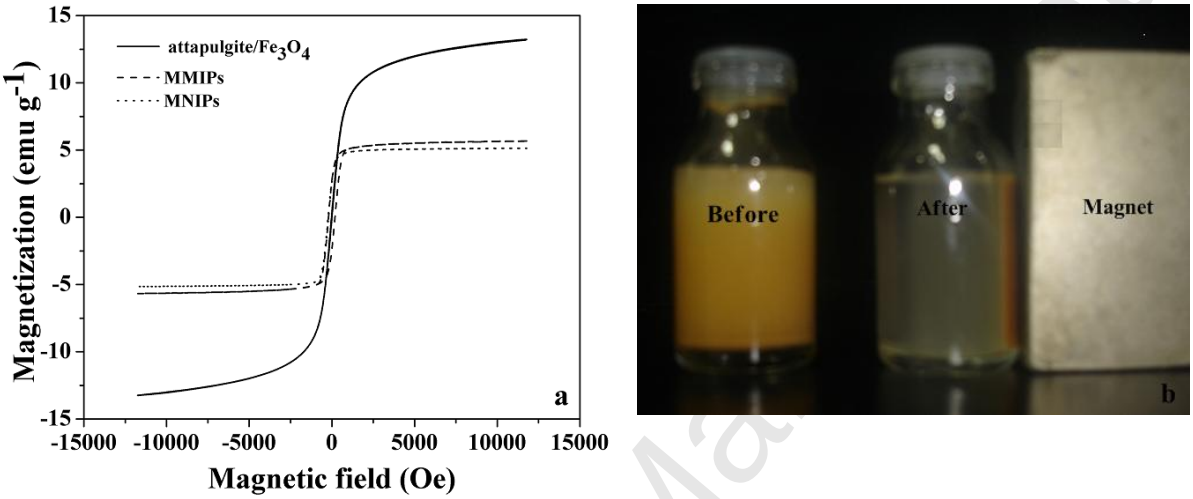

Fig. 5 (a) Magnetization curves at 298K of ATP/Fe_3O_4, MMIPs and MNIPs. (b) A photograph of MMIPs suspended in water in the absence (left image) and in the presence (right) of an externally placed magnet.

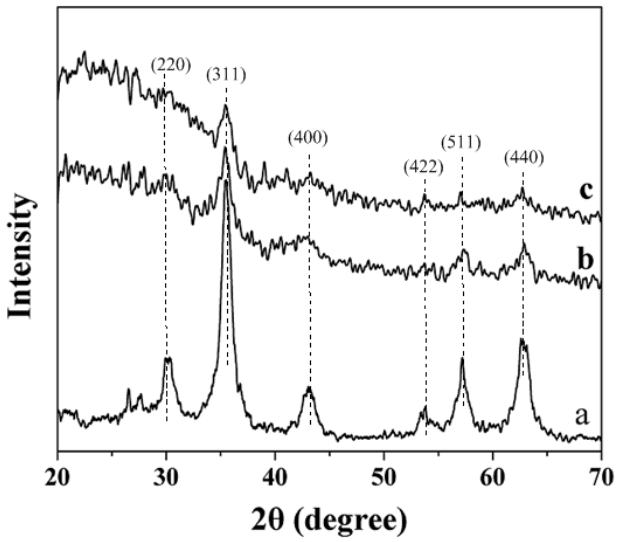

Fig. 6 X-ray diffraction (XRD) patterns of ATP/Fe_3O_4 (a), MMIPs (b) and MNIPs (c).

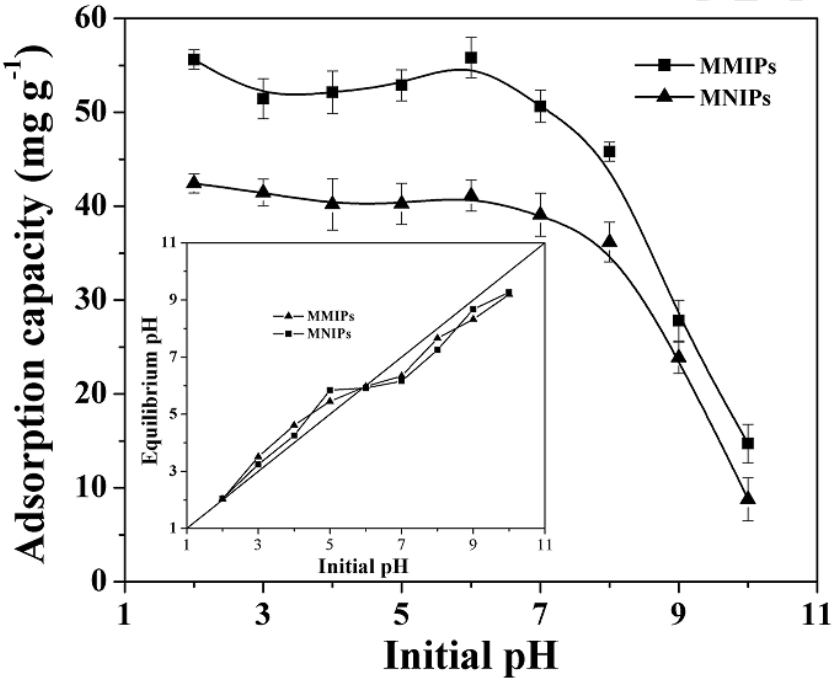

Fig. 7 Effect of pH on adsorptive removal of 2,4-DCP. Inset: Effect of initial pH on equilibrium pH.

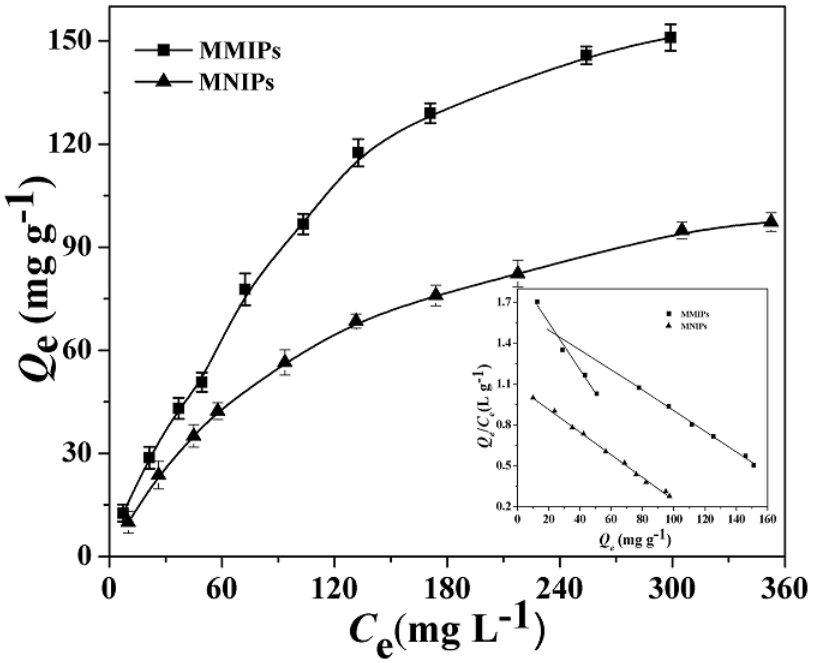

Fig. 8 The adsorption isotherms and the Scatchard plots of MMIPs and MNIPs (inset).

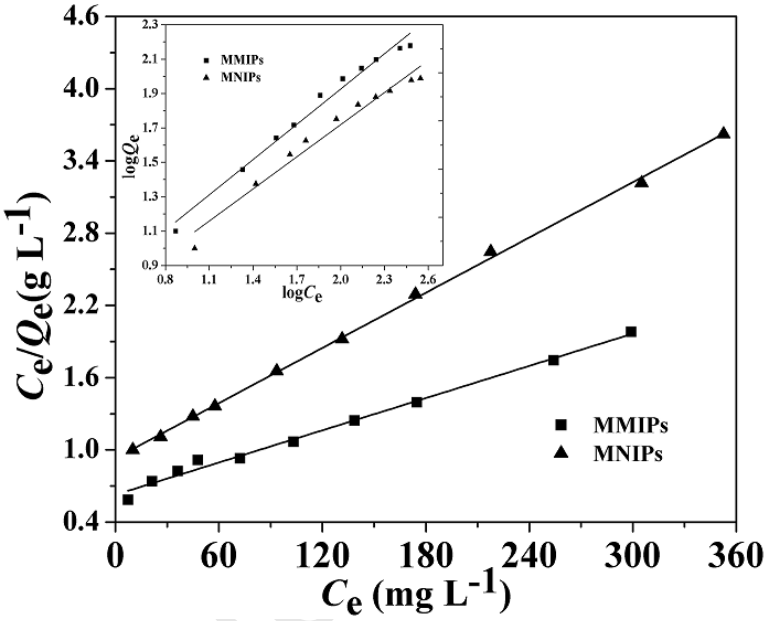

Fig. 9 Fitting the experimental data with Langmuir and Freundlich (inset) isotherm equations.